

Preliminary Results, Analysis, and Overview of Part -1 of the GOLD Experiment

K.E. Wilson, M. Jeganathan

Jet Propulsion Laboratory, California Institute Of Technology

ABSTRACT

The Ground/Orbiter Lasercomm Demonstration (GOLD) is an optical communications demonstration between the Japanese Engineering Test Satellite (ETS-VI) and an optical ground transmitting and receiving station at the Table Mountain Facility, Wrightwood California. Laser transmissions to the satellite were performed approximately four hours every third night when the satellite was at apogee above Table Mountain. The experiment required the international coordination of resources to generate and transmit real-time commands and to receive telemetry from the ETS-VI. Participating organizations included CRI, JPL, NASDA's Tsukuba tracking station and NASA's Deep Space Network at Goldstone, CA. Transmissions to the ETS-VI began in November 1995 and lasted until January 13, 1996, when, for a major part of its orbit, the satellite became eclipsed by the Earth's shadow. There are no laser transmissions during the eclipse. Post-eclipse experiments are currently being negotiated.

1. INTRODUCTION

The Ground/Orbiter Lasercomm Demonstration (GOLD) is a joint NASA/CRI (Communications Research Laboratory) optical communications experiment with the ETS-VI satellite to evaluate 1-way and 2-way optical communications under a range of atmospheric conditions. The ETS-VI was launched August 28, 1994, and was to be placed in a geo-stationary orbit above Japan. Difficulty with one of its motors resulted in the satellite being left in a geo-transfer orbit. This unfortunate occurrence, however, made the satellite visible from ground stations around the world and researchers at the CRI encouraged NASA experimenters to use the optical communications subsystem on board the satellite. GOLD is NASA's response to this invitation. NASDA engineers adjusted the satellite's orbit to facilitate the use of the Laser Communications Equipment (LCE) by experimenters at JPL. Phase-I began in November 1995 and lasted to mid-January 1996. The satellite then went into a two-month-long eclipse between mid-January and mid-March, and no experiments were conducted during the eclipse. As of this writing, NASDA is continuing to monitor the power generation capabilities of the satellite to assess the feasibility of post-eclipse experiments.

The concept of the GOLD project is shown in Figure 1.1. The transmitter was a 0.6-m telescope located at NASA's Table Mountain Facility (TMF), and the receiver was a 1.2-m bent-Cassegrain telescope located approximately 60-m from the transmitter. The primary uplink signal was a 1.024 Mbps Manchester-coded PN sequence to the spacecraft. For the downlink, the ETS-VI used its AlGaAs laser to transmit a similar PN sequence to the 1.2-m ground receiver. This paper describes the work on GOLD Phase-I. The transmitter and receiver stations are discussed in Section 2. Experiment results are presented in Section 3, and Conclusions and Acknowledgments are in Sections 4 and 5.

2. THE GOLD GROUND STATIONS

The GOLD experiment was performed when the satellite was near apogee and above TMI. Figure 2.1 shows the satellite's ground track in its three-day sub-recurrent orbit. The darkened section of the trajectory in the figure shows the part of the orbit when the experiment is performed. During this time the satellite is at zenith over Central America. Pointing the downlink laser beam to the ground station is accomplished using a combination of satellite attitude and LCI's gimbal controls. As the figure shows, this pass occurs approximately 14 hours after the pass over Tokyo. This opportunity was used by the TMI team to learn about the satellite and LCI's performance before the TMI pass. Transmission to the satellite on intermediate days when apogee occurred over the Hawaiian Islands was precluded by field-of-view and bias pointing constraints on the satellite and its detectors.

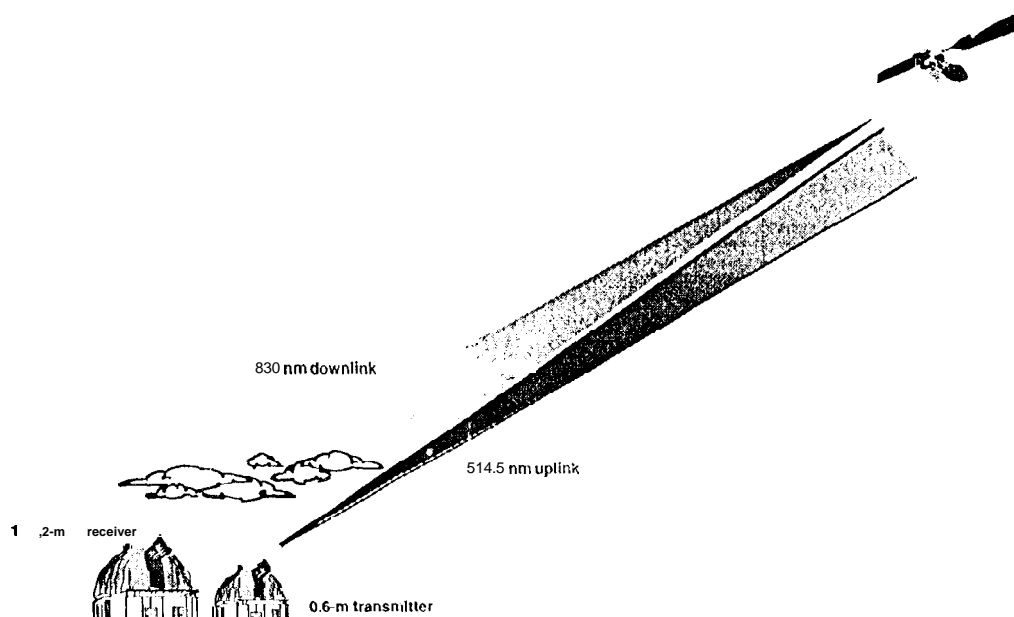


Figure 1.1: Conceptual drawing of GOLD. Transmitter at TMI uplinks 514.5 nm communications signal to HTS-VI spacecraft. Satellite downlinks 830 nm 1 Mbps signal

2.1.1 The Transmitter

The transmitter consisted of an Argon-ion laser coupled to the 0.6-m telescope at TMI. The telescope is located in building TM-12 at TMI; its surveyed position is:

Longitude	117°40' 52.55"
Latitude	34°22' 53.49"
Altitude	2,286 km

The telescope was operated in the coudé mode that allowed coupling in of light from the large high power laser. The uplink laser was a prism tuned Coherent Innova-100 Ar-Ion that delivered a maximum of 14.5 Watts linearly polarized output power at 514.5 nm. Because the laser output was spatially multimode at maximum power, it was operated below maximum (typically 13 Watts) to achieve good beam quality. Coalignment of the laser beam with the telescope axis was achieved by adjusting the position of the

telescope's secondary mirror until the focus was brought to a position on the optical bench. At this setting the telescope's focal ratio was $f/41$, (that is a focal length of 26.4 -m).

A schematic of the optical train is shown in figure 2.1.1.1, An electro-optic modulator was used to impress the uplink data stream on the optical carrier. The modulator consisted of four KD*P crystals and a polarizer. A data formatter - a 1 'irebird 6000 bit-error-rate tester (BERT)-generated a 0 to 1 volt modulation pattern that was amplified to the modulator's half-wave voltage and applied to the crystals.

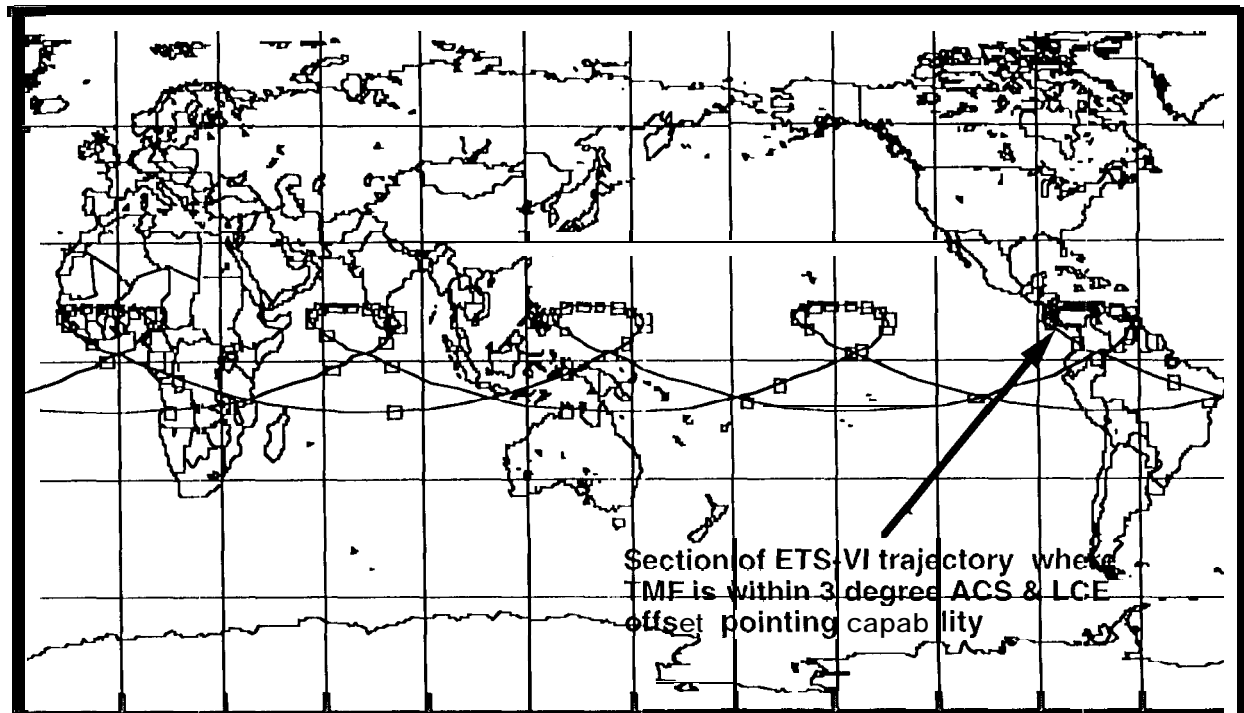


Figure 2.1: 1 ETS-VI ground track showing the section (darkened area) where combined LCE and satellite ACS satellite pointing capabilities could support optical communications experiments from TMF. The track covers November 26-29, 1995. The markers are one hour time spans.

After modulation, the beam was incident on a concave/convex lens pair that set the beam divergence out of the telescope; this typically ranged from 20 urad to 40 urad. To mitigate the effects of atmospheric scintillation on the uplink beacon, the output beam was split into two equal parts. One beam was sent through a 25 cm optical delay line; a path length difference greater than the laser's 10 cm coherence length. Both beams were then reflected from a high power dichroic beam-splitter and were brought to a focus at the iris located at the $f/4$ focus of the telescope. From there the beams diverged and were reflected by the third coude flat and into the telescope. The beams were arranged to be incident on opposite sides of the 0.6-m telescope's primary mirror, a distance greater than the size of an atmospheric coherence cell.

imaging the satellite was done using a Pulnix camera with image intensifier that extended the detection capability down to 10^{-6} lux. This enabled us to track the satellite around apogee where, depending on the phase angle of the solar panels, its brightness varied from that of a magnitude 12 to a magnitude 14 star. The avalanche photodiode (APD) transmit detector monitored the modulation of the transmitted signal.

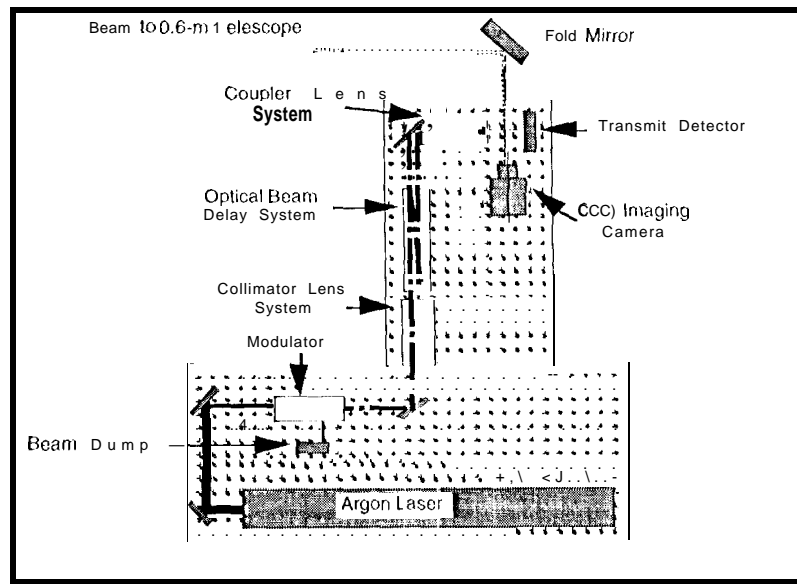


Figure 2.1.1.1: This schematic of optical train for GOLD experiment shows laser, the modulator, and the optical beam delay system used to provide temporal and spatial diversity of the optical beams transmitted to the satellite. The detector that was used to monitor the modulated wave form and the CCD camera for imaging the satellite are also shown.

2.1.2. The Receiver

The receiver consisted of an optical detection package that weighed approximately 30 kg attached to a 1.2-m (f/29.5) telescope. The detection package was mounted to the telescope's bent Cassegrain focus, and consisted of two CCD cameras and a 3-mm diameter low-noise APD. See Figure 2.1.2.1. The cameras were a wide-field Cohu with image intensifier for satellite acquisition and tracking, and a Spectra Source CCD for making atmospheric seeing measurements. The detectors were coaligned on a rigid optical bench assembly to ensure that the downlink transmission remained incident on both the tracking and communications detectors as the telescope tracked the satellite across the sky.

Satellite acquisition at the receiver station was accomplished by using a series of steps. It began with calibrating the pointing direction of the narrow field-of view 1.2-m telescope with that of a wide field 0.4-m guiding telescope attached to the 1.2-m telescope's frame. Coalignment was accomplished by first acquiring a bright star in the guiding telescope and then adjusting the pointing of the receiver telescope until the star was observed in the 1.2-m telescope. The blind point accuracy of the telescope depended on separation between the calibration star and the satellite positions. The telescope was therefore moved to a star in the vicinity of the satellite and the pointing offsets noted for calibration. The large dynamic range between the calibration stars (3^{rd} to 5^{th} magnitude) and the satellite (-12^{th} to -14^{th} magnitude) was compensated for by using a #2 optical density filter in an electronically-switched filter holder located in front of the tracking. The filter was placed in the optical beam during the calibration and was switched out for satellite acquisition.

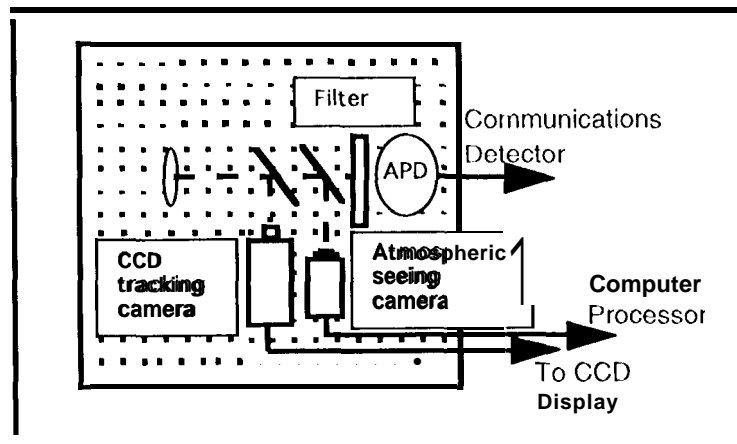


Figure 2.1.2.1: Schematic of optical receiver located at focus of 1.2-m telescope. CCDs detectors in the optical train track the satellite and measure atmospheric seeing. The APD detects the 1.024 Mbps optical downlink data stream.

Atmospheric seeing measurements were made to validate our theoretical models that predict the effects of **scintillation** on the **optical** uplink. The seeing data were taken at 15 minute intervals to provide an accurate correlation between the atmospheric seeing and the observed uplink scintillation.

Downlink data recovery electronics began with the APD amplifier and signal conditioner. The satellite downlink data sequence was in one of three formats: (i) 1.024 Mbps PN, (ii) real-time telemetry at 128 kbps with each bit repeated 8 times to produce a 1.024 Mbps data rate, and (iii) regenerated uplink square wave at 1 MHz. All data streams except the square wave modulation were Manchester coded. The amplified APD output was processed to provide both an analog and a digital output of the downlinked data stream. The digital output was bit-synchronized and stored on a data recorder for future processing. The analog data were displayed on a digital storage oscilloscope and segments stored on disk. A segment of the PN downlinked analog data stream showing the characteristic random bit-flips is seen in figure 2.1.2.2.

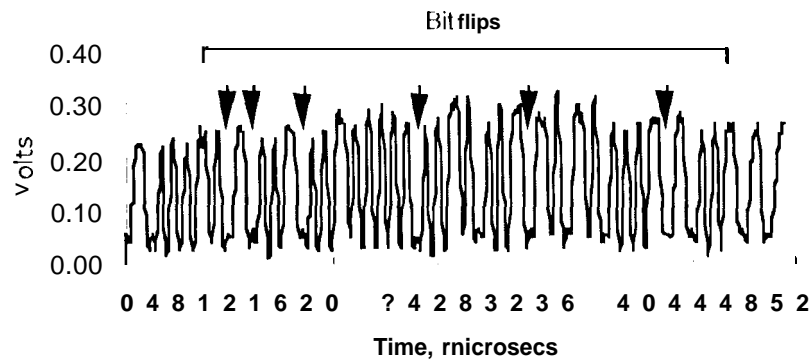


Figure 2.1.2.2: Sample of 1.024 Mbps Manchester-coded PN sequence downlink data-stream from ICB showing random bit flips. A few of these are indicated by arrows.

3. EXPERIMENT RESULTS AND DATA ANALYSIS

There were twenty-six satellite passes over TMI (a satellite transmission pass was scheduled every third day) during the period October 30, 1995, to January 13, 1996. The passes were initially about 3 hours

in duration; this was increased to about 5 hours after the November 25 satellite maneuver. Experiments on Thanksgiving, Christmas and New Years holidays were canceled to allow team members to be with their families. Of the passes canceled five were due to inclement weather, one was due to a telescope scheduling conflict, and two were due to unavoidable equipment anomalies. The first two operational passes were used to shake out the ground telescope systems and to learn how to coordinate remotely with the CRL satellite controllers. No signal detections were observed on those nights. On the 13 remaining passes, both uplink and downlink signal detections were observed. Uplink signal detection was confirmed by monitoring the voltage levels on the spacecraft's CCD and QD optical communication terminal's tracking detectors. Telemetry readings of these voltage levels were radio-transmitted to the ground, processed by CRL and transmitted over communications lines to U'able Mountain. These data were sampled at intervals of one second and the latency of the data upon arrival at TMF was about 15 seconds.

To reduce the effects of uplink turbulence, we used a dual uplink beam approach where half of the power was placed into each of two spatially separated uplink beams. The beams combined in the far field to produce a full-power signal, but since the beams were in independent turbulence regions of the uplink telescope, there was averaging of the turbulence effects. The improvement due to this multi-beam averaging was included in the analysis. The two-beam uplink data were fit to an appropriately-scaled log-normal distribution and the resulting distribution was compared with the theoretically estimated distribution generated a-priori. The results of this comparison are shown in Figure 3.1. These curves clearly show an improvement due to the two-beam approach. A comparison of the theoretical and experimental results shows that the standard deviation (S.D) of the (distribution for the fitted results are extremely close to that predicted by the two-beam theory.

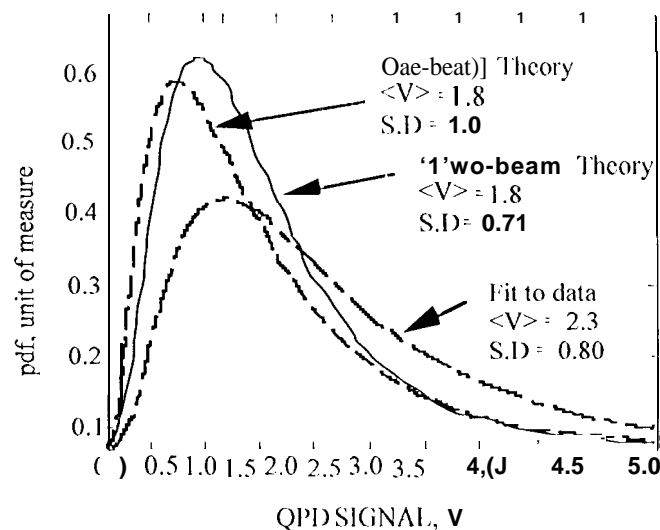


Figure 3.1: Theoretically predicted probability density functions for one and two beam uplinks are compared with the fitted curve from the GO1.11 uplink data. The theory, which does not include the effects of uplink pointing jitter, agrees reasonably with the experimental data.

1 histograms of the measured intensity levels for one-beam and two-beam uplinks are shown in Figures 3.2 (a) and 3.2 (b). The data in each of these plots represents approximately 1200 data points taken over a twenty minute period. A comparison of the two figures shows the advantage of two-beam over a one-beam uplink. Figure 3.2 (a) shows that pointing and beam wander effects result in a large number of low signal strength detections. The figure also shows a suggestion of a second maximum (occurring at about 1/7 of the frequency) at higher (around 2.0) levels. Figure 3.2 (b) shows a similar low signal peak as the one-beam. However, this occurs at less than 1/2 the frequency of that of Figure 3.2 (a), and is

comparable in frequency to the peak in the distribution (around 2.5). Our preliminary interpretation of these data is that because the two beams are propagating through different atmospheric cells they wander independently and randomly. The net effect is thus a reduction in the frequency and depth of the signal fades at the satellite. These effects will be investigated in greater detail in Phase-II.

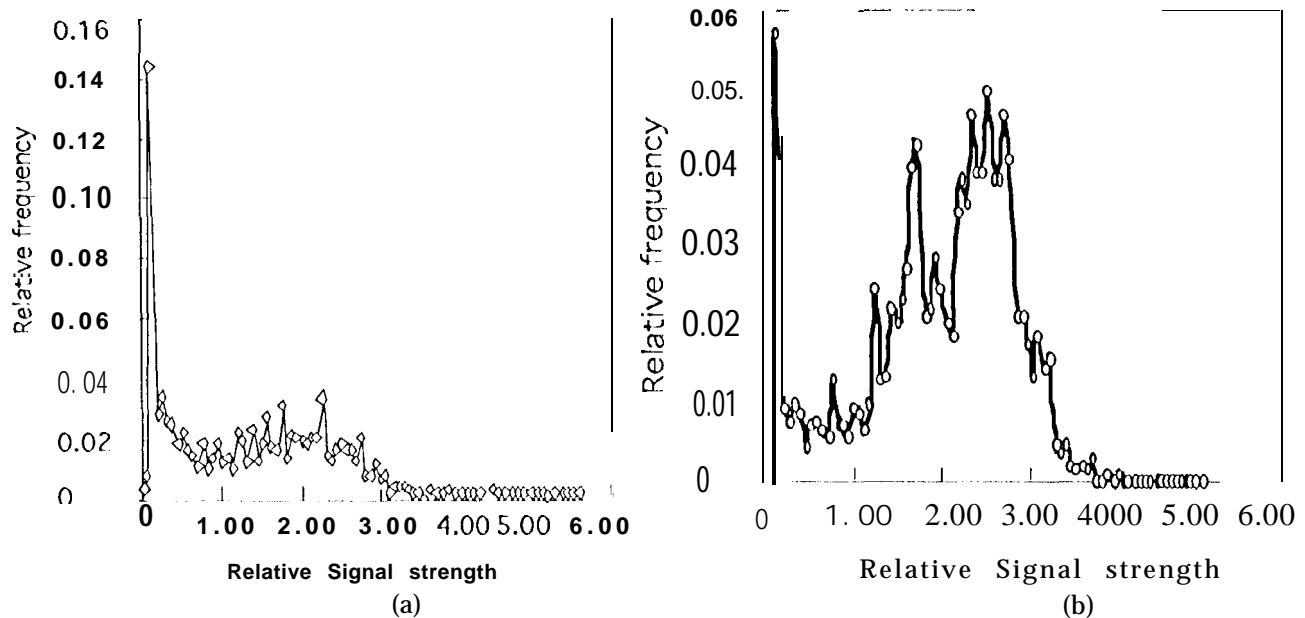


Figure 3.2: Histograms of detected signal strength for one-beam (a) and two-beam (b) uplink transmissions as detected by the QD optical detector in the LCE show the advantage of two-beam uplink transmission.

4. CONCLUSIONS

GOJ11 was an experiment that demonstrated real-time international collaboration. It demonstrated the first optical signal regeneration between a satellite and an optical ground receiver. The experiment also demonstrated the advantages of multi-beam uplink transmission. The thrust of the phase-1 experiment was to measure and understand the performance of the 2-way optical link under a variety of atmospheric attenuation and turbulence conditions. The data accumulated from this experiment will enable us to improve our theoretical models and to better define the performance of the technology for mission designers who are interested in optical communications for future missions. Satellite ranging using regeneration of an uplinked code is a time-tested approach in rf communications systems. A post-eclipse GOJ11 opportunity will allow us to investigate this approach at optical frequencies.

5. ACKNOWLEDGMENTS

The authors would like to acknowledge all of our fellow GOJ11 team members at the CRJ., JPL., NAS1 DA and the DSN. Their commitment and diligence made it possible to design procure and assemble the subsystems needed to convert the two 'T'M F astronomical facilities into optical communications facilities in the short period of only four months.

The work described in this paper was performed by the Jet Propulsion Laboratory, California Institute of Technology, under contract with the National Aeronautics and Space Administration.